BULETINUL INSTITUTULUI POLITEHNIC DIN IAȘI
Publicat de
Universitatea Tehnică „Gheorghe Asachi” din Iași
Volumul 62 (66), Numărul 1, 2016
Secția
ELECTROTEHNICĂ. ENERGETICĂ. ELECTRONICĂ

SINGLE-PHASE AC-AC CONVERTER

BY

OVIDIU URSARU[*] and CRISTIAN AGHION

Technical University “Gheorghe Asachi” of Iași,
Faculty of Electronics,Telecommunications and Information Technology

Received: February 10, 2016
Accepted for publication: February 29, 2016

Abstract. This paper presents a direct AC-AC single-phase buck-boost converter. The circuit is simple and has good performances, whatever the load nature. The correct functioning of the circuit at a 20 kHz switching frequency was tested both by simulation and experimentally.

Key words: choppers; power conversion; circuit simulation.

1. Introduction

AC-AC converters are currently used in numerous fields, such as: AC motor drive, adjustable AC power supplies, electronic transformers, voltage waveform restorers, adjustable impedances, etc. These converters successfully replace alternating voltage variators using thyristors or triacs. Since the functioning frequency is high (more than 20 kHz), there is no noise, filters are small in size, efficiency is high and the current from the power supply is nearly sinusoidal.

The first AC-AC converters analysed were buck converters (AC choppers) (Revenkar, 1977). References (Chose & Park, 1989; Jang & Choe, 1991; Do-Hyum & Choe, 1995) present improved PWM techniques, which increase the power factor and eliminate certain harmonics (in the absence of grid filters). In (Lucanu & Ursaru, 2003), simulations were used to analyse an

[*]Corresponding author: *e-mail*: ovidiu@etti.tuiasi.ro

IGBTs chopper at a 5kHz frequency. Reference (Congwei & Bin, 2009) presents a three-phase AC-AC converter with 9 IGBTs, and (Lai & Wang, 2009) suggests an evaluation method for three-phase AC converters.

In Lucanu & Ursaru (2005) and Kim & Min (1998), the choppers presented have improved switching and increased efficiency, but the circuits are complex. References Li & Yang (2001) and Thiago & Clovis (2011) present AC choppers with three-level converters and topologies that use commercial power modules (Neascu, 2013). In Aghion & Lucanu (2012) a high-performance AC-AC single-phase converter with two inductances and four IGBTs is presented.

This paper presents a direct AC-AC single-phase buck-boost converter using two IGBTs, eight diodes, an inductance and a capacitor (except for the grid filters). In fact, it is a classic buck-boost converter structure, where the two switches used are AC switches and a grid filter was added. The converter functions adequately irrespective of the load nature and it can insure a bidirectional energy flow if the load contains an AC source. The circuit design equations are presented below. The adequate functioning of the converter is checked both by simulation and experimentally; the tests were applied to a converter prototype developed by the authors. The prototype was used for connecting a device to the grid, when the nominal power supply is different of nominal voltage load.

2. Circuit Analysis

Fig. 1 presents the circuit of the AC-AC single-phase buck-boost converter.

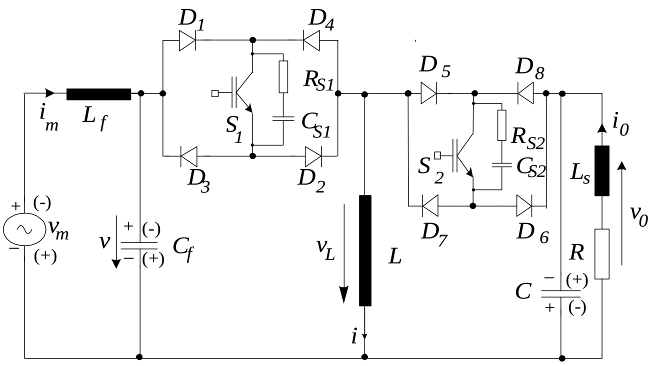

Fig. 1 – Single-phase direct ac-ac buck-boost converter.

The AC-AC converter contains the grid filter L_f, C_f, the inductor L, the capacitor C connected in parallel with the load impedance R, L_S and two AC switches: one of them is made up of the IGBT S_1 and the diodes D_1-D_4, and the other one includes S_2 and D_5-D_8. The snubber circuits R_{S1}, C_{S1} and R_{S2} C_{S2} are connected in parallel with the IGBTs.

Fig. 2 shows the waveform of the voltage v at the C_f capacitor terminals, and the generation of the control signals for the IGBT's S_1 and S_2. If the current through the inductor L is $i > 0$, for time intervals [0, DT], it will flow through D_1, S_1, D_2, L. The load resistor R is powered by the capacitor C. For time intervals [DT, T], the current i will flow through L, the R-C circuit, D_6, S_2, D_5.

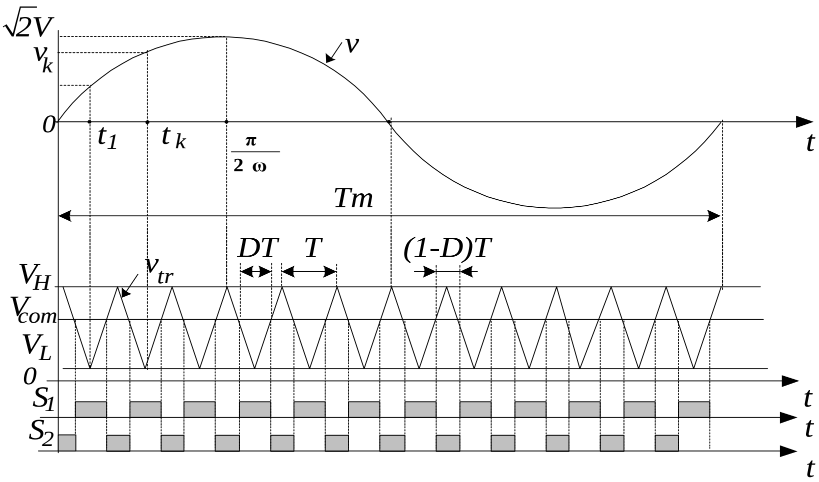

Fig. 2 – The waveform of the v voltage and the generation of the control signal for IGBT's.

We used uniform PWM control (Barleanu & Baitoiu, 2012), in which the conduction durations for the two switches are the same in all switching periods T, as in DC converters, and $f = 1/T$ is the switching frequency (Valachi & Timis, 2009). The equations that describe the functioning of the converter rely on the following simplifying hypotheses: the passive components are ideal, the power devices are ideal switches, the voltage V on the capacitor C_f and the voltage V_0 on the load are sinusoidal and remain constant for a period T, and the load is purely resistive. If V_k and V_{k0} are voltages from the middle of the switching period K and ω is the grid voltage frequency, we can write the following equations:

$$\begin{cases} v = \sqrt{2}V\sin\omega t, \\ v_K = \sqrt{2}V\sin\omega t_K = \text{ const., } t_K(k-1)T + \dfrac{T}{2}, \\ v_{0K} = \sqrt{2}V_0\sin\omega t_K = \text{ const.} \end{cases} \tag{1}$$

For the interval [0, DT], when S_1 is conducting and S_2 is off:

$$\begin{cases} v_{LK} = L\dfrac{\mathrm{d}i_K}{\mathrm{d}t} v_K, \\ i_K = I_{Km} + \dfrac{v_K}{L} t. \end{cases} \tag{2}$$

By replacing $t = DT$ to the eq. (2), we get the ripple of the current i through the inductor L in the switching period K:

$$\begin{cases} i_K = I_{KM} = I_{Km} + \dfrac{v_K}{L} DT, \\ \Delta i_K = I_{KM} - I_{Km} = \dfrac{D}{Lf} v_K. \end{cases} \tag{3}$$

For the interval $[DT, T]$, when S_1 is off and S_2 is conducting:

$$\begin{cases} v_{LK} = v_{0K}, \\ i_K = I_{KM} - \dfrac{v_{0K}}{L} t', \;\; t' \in [0, (1-D)T]. \end{cases} \tag{4}$$

Since this is a buck-boost converter, the control characteristic corresponding to the switching period K can be approximated by the equation below:

$$v_{0K} = \frac{D}{1-D} v_K. \tag{5}$$

In a similar way we obtain the following average values of the currents through the bidirectional switches, corresponding to the switching period K:

$$\begin{cases} I_{S_1K} = \left(\dfrac{D}{1-D}\right)^2 \dfrac{v_K}{R}, \\ I_{S_2K} = \dfrac{D}{1-D} \cdot \dfrac{v_K}{R}. \end{cases} \tag{6}$$

and the following values for the maximum repetitive currents:

$$I_{S_1KM} = I_{S_2KM} = I_K + \frac{\Delta i_K}{2} = \frac{Dv_K}{(1-D)^2 R} + \frac{Dv_K}{2Lf}. \tag{7}$$

The maximum collector-emitter voltages on the two IGBTs in the switching period K are the following:

$$V_{S_1KM} = V_{S_2KM} = v_{0K} = \frac{Dv_K}{1-D}. \tag{8}$$

The voltages V_K have sinusoidal variation, therefore the average values of the currents through the switches on a period *Tm* of the *AC* grid voltage are:

$$\begin{cases} I_{S_1\text{avr}} = \left(\dfrac{D}{1-D}\right)^2 \dfrac{2\sqrt{2}V}{\pi R}, \\ I_{S_2\text{avr}} = \dfrac{D}{1-D} \cdot \dfrac{2\sqrt{2}V}{\pi R}. \end{cases} \tag{9}$$

and the maximum repetitive currents are:

$$I_{S_1M} = I_{S_2M} = \frac{D\sqrt{2}V}{(1-D)^2 R} + \frac{D\sqrt{2}V}{2Lf}. \tag{10}$$

The IGBT's stress voltage is:

$$V_{S_1M} = V_{S_2M} = \frac{D\sqrt{2}V}{1-D}. \tag{11}$$

The normalised current ripple results from equations (3) and (6):

$$\frac{\Delta I_k}{I_K} = \frac{(1-D)^2 R}{Lf}. \tag{12}$$

This equation can be used for calculating the inductor *L*. The normalised ripple of the output voltage can be calculated by:

$$\frac{\Delta v_0}{v_0} \approx \frac{1-D}{RCf}. \tag{13}$$

This equation allows for the calculation of the value of the capacitor *C*.

3. Simulation and Experimental Results

The adequate functioning of the circuit was tested by simulation and experimental prototype. The load used in the simulations and in the prototype is the same - a resistive load: R = 390 Ω, inductive load L_S =750 mH, R = 390 Ω and the switching frequency is f = 20 kHz.

Table 1 shows the main parameters used for the simulations and the experimental prototype.

Table 1
Key Parameters of Experimental Prototype

Parameters	Symbol	Value
AC input voltage	V_m	110 V (RMS)
Input frequency	f_m	50 Hz
Resistive load	R	150 Ω
Inductive Load	R/L_s	150 Ω/750 mH
Transistors	S_1, S_2	IRGB8B60KPBF
Diodes	D_1-D_8	MUR460
Capacitor	C	2 uH
Input filter	L_f	13 mH
	C_f	10 uF
Microcontroller		PIC16F684
Snubber	$R_{S1\text{-}S2}$	100 Ω
	$C_{S1\text{-}S2}$	3.3 nF

Fig. 3 shows the waveforms obtained by simulations, - the waveforms of the i_0 current load and of the i_m current source and the waveforms of the v_0 voltage load and of the v_m voltage source and for a duty factor D = 0.3.

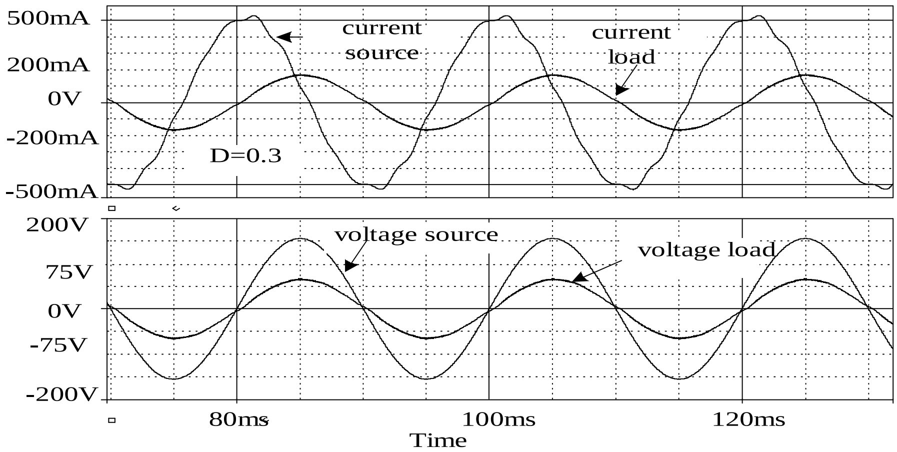

Fig. 3 – Waveforms of the i_m current, i_0 current and v_m voltage, v_0 voltage for D = 0.3, in the resistive load case R = 150 Ω.

Fig. 4 show the same waveforms for D = 0.3, for the inductive load case, where the output impedance is: R = 150 Ω and L = 750 mH.

Fig. 5 shows the waveforms obtained by simulations, namely the waveforms of the i_0 current load and of the i_m current source and the waveforms of the v_0 voltage load and of the v_m voltage source and for a duty factor D = 0.7.

Fig. 6 show the same waveforms for D = 0.7, for the inductive load case, where the output impedance is: R = 150 Ω and L = 750 mH.

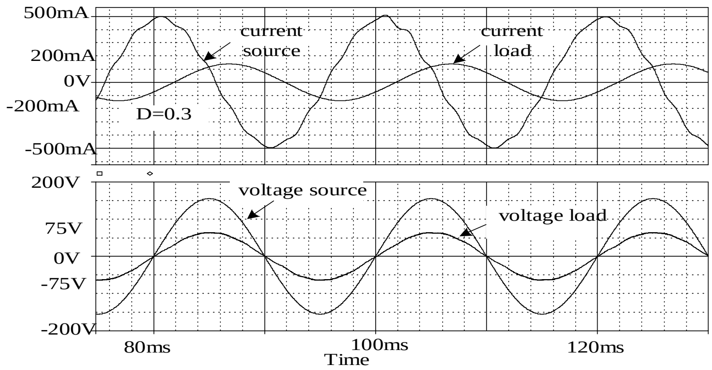

Fig. 4 – Waveforms of the i_m current, i_0 current and v_m voltage, v_0 voltage for D = 0.3, in the inductive load case (L = 750 mH and R = 150 Ω).

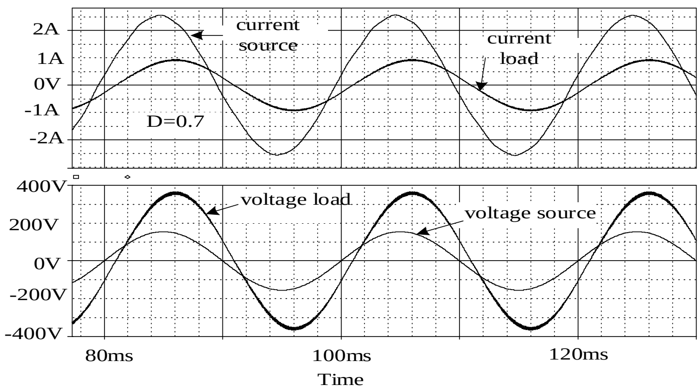

Fig. 5 – Waveforms of the i_m current, i_0 current and v_m voltage, v_0 voltage for D = 0.7, in the resistive load case R = 150 **Ω**.

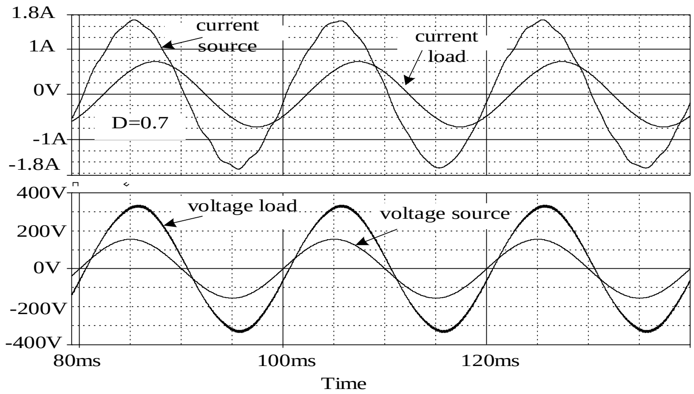

Fig. 6 – Waveforms of the i_m current, i_0 current and v_m voltage, v_0 voltage for D = 0.7, in the inductive load case (L = 750 mH and R = 150 Ω).

As presented in Fig. 7, the prototype circuit is made up of two boards; one of them includes the microcontroller, the *LCD*, the drivers and the low-voltage supply circuit, and the other one contains the proposed power circuit, based on the schematic presented in Fig. 1.

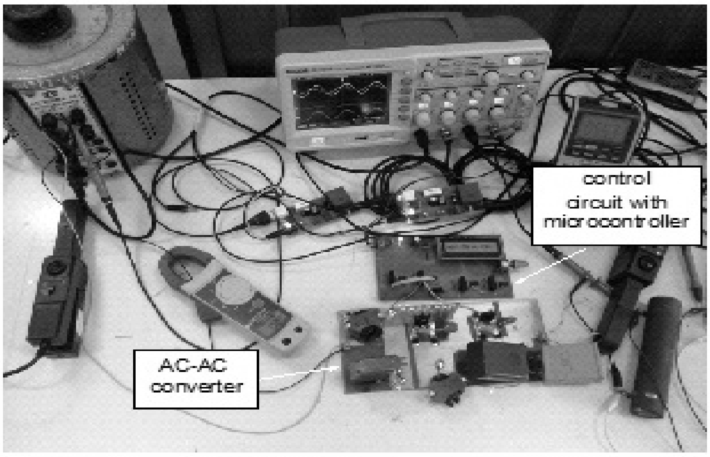

Fig. 7 – Experimental setup.

Fig. 8 shows the waveforms obtained by measurements, the waveforms of the i_0 current load and of the i_m current source and the waveforms of the v_0 voltage load and of the v_m voltage source and for a duty factor D = 0.3.

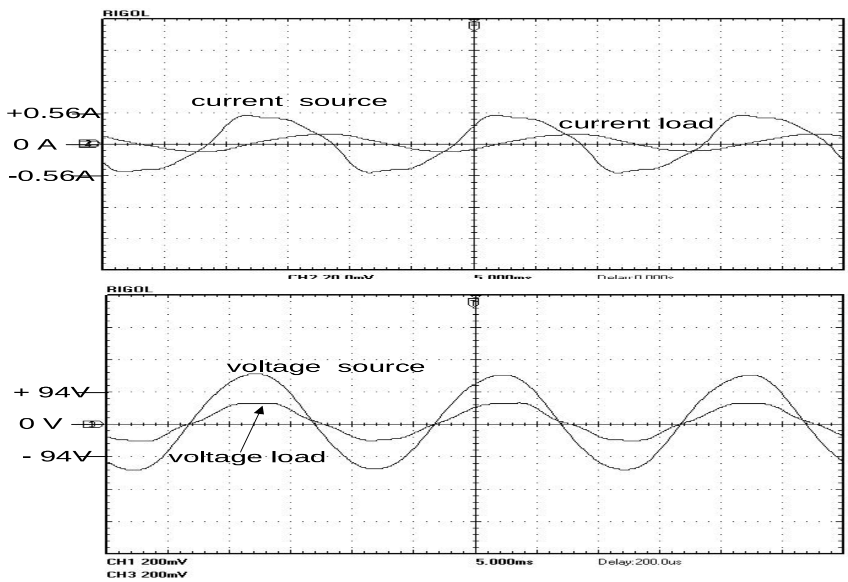

Fig. 8 – Waveforms of the i_m current, i_0 current and v_m voltage, v_0 voltage for D = 0.3, in the resistive load case R = 150 Ω.

Fig. 9 show the same waveforms for D = 0.3, for the inductive load case, where the output impedance is: R = 150 Ω and L = 750 mH.

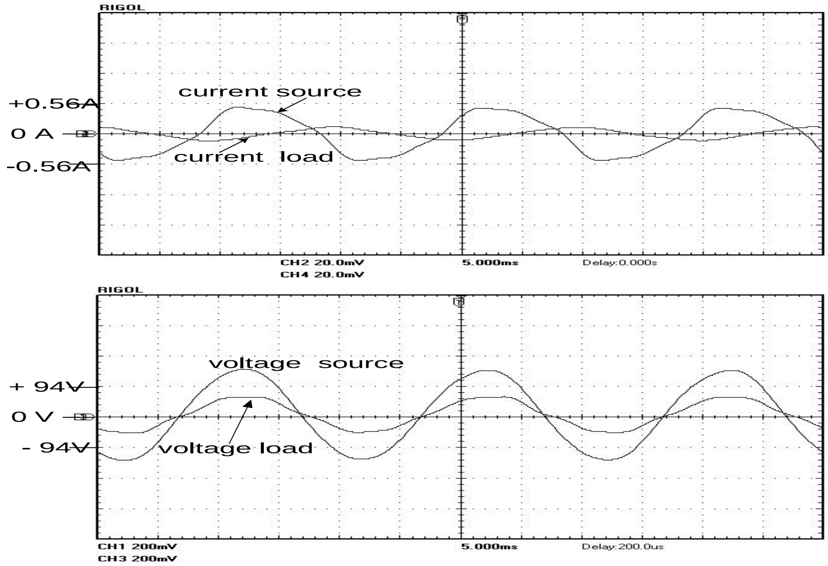

Fig. 9 – Waveforms of the i_m current, i_0 current and v_m voltage, v_0 voltage for D = 0.3, in the inductive load case (L = 750 mH and R = 150 Ω).

Fig. 10 shows the waveforms obtained by measurements, the waveforms of the i_0 current load and of the i_m current source and the waveforms of the v_0 voltage load and of the v_m voltage source and for a duty factor D = 0.7.

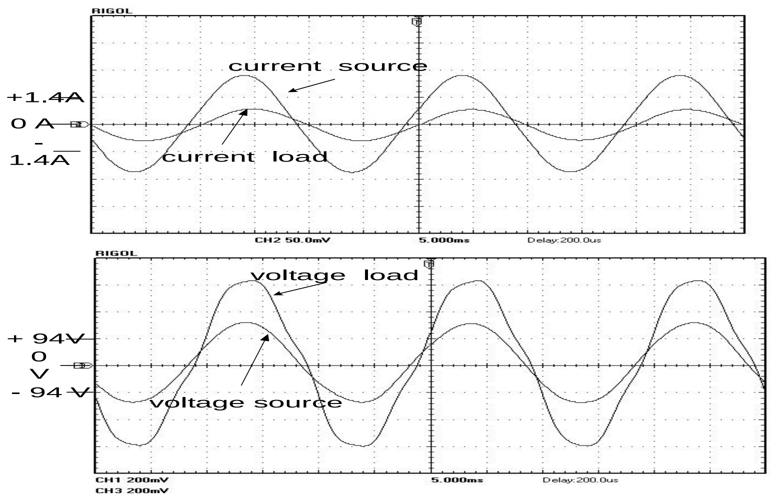

Fig. 10 – Waveforms of the i_m current, i_0 current and v_m voltage, v_0 voltage for D = 0.7, in the resistive load case R = 150 Ω.

Fig. 11 show the same waveforms for D = 0.7, for the inductive load case, where the output impedance is: R = 150 Ω and L = 750 mH.

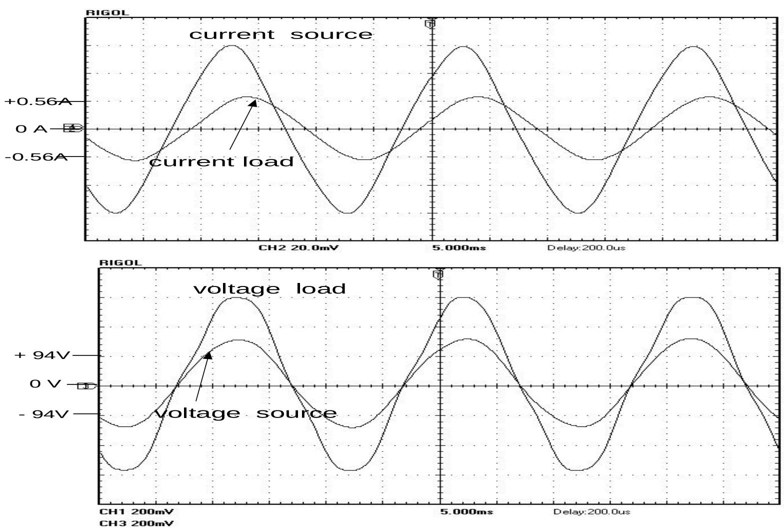

Fig. 11. Waveforms of the i_m current, i_0 current and v_m voltage, v_0 voltage for D = 0.7, in the inductive load case (L = 750 mH and R = 150 Ω).

Fig. 12 *a* shows *THD* for the input current obtained by simulations and measurements for resistive load and Fig. 12 *b* shows *THD* for the input current obtained by simulations and measurements for inductive load.

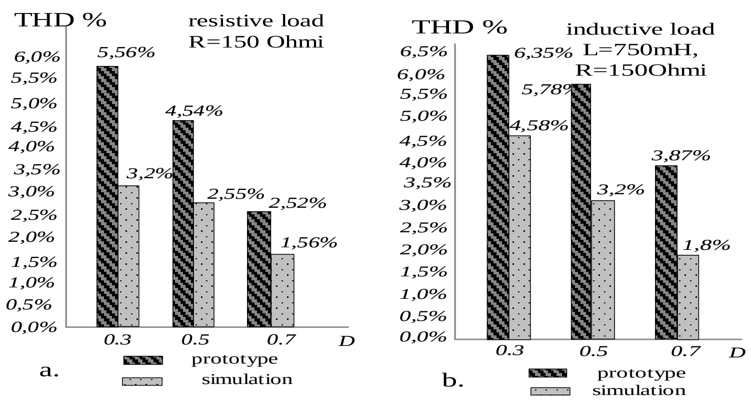

Fig. 12 – THD analysis for the input current: *a* – for the resistive load, *b* – for inductive load.

Fig. 13 *a* shows the efficiency obtained by simulations and measurements for the cases of the resistive load, Fig. 13 *b* shows the efficiency obtained by simulations and measurements for the cases of the inductive load.

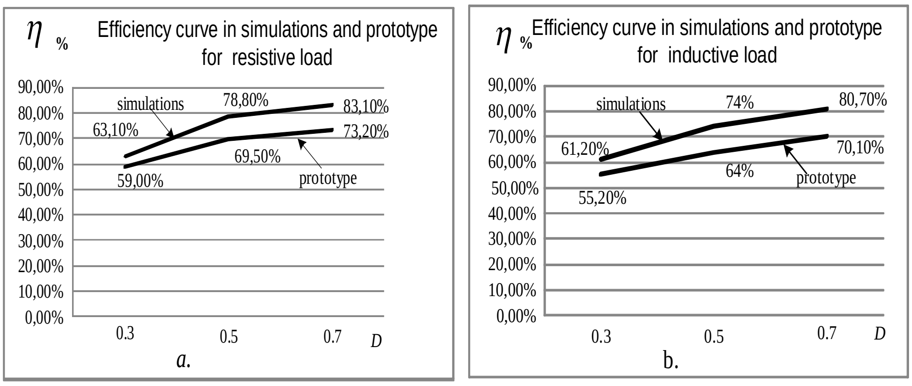

Fig. 13 – Efficiency: *a* – for the resistive load, *b* – for the inductive load.

4. Conclusions

The paper presents a direct AC-AC buck-boost converter circuit containing, beside the grid filter, two bidirectional current switches, each made up of one IGBT, four diodes and a boost inductance.

Switches were controlled by uniform sampling, with the same duty cycle in all the switching periods. The resulting control circuit is simple and the energy flow can be bidirectional. The adequate functioning of the circuit was tested by simulation, as well as on a laboratory prototype

The results allowed the identification of the control characteristic and of the functioning efficiency. The waveforms obtained for the load voltage and current are very good. The supplied current is sinusoidal, therefore the circuit can be used particularly for converting the RMS voltage from 110 V to lower voltage or upper voltage depending of the duty cycle D.

REFERENCES

Aghion C., Lucanu M., Ursaru O., Lucanu N., *Direct AC-AC Step-Down Single-Phase Converter with Improved Performances.* Electronics and Electrical Engng., **18**, *10*, 33-36 (2012).

Bârleanu A., Băiţoiu V., Stan A., *FIR Filtering on ARM Cortex-M3.* Proc. of the 6th WSEAS European Computing Conf., *9*, 2012, WSEAS Press, 490-494.

Chose G., Park M., *An Improved PWM Technique for AC Chopper*. IEEE Trans. on Power Electronics, **4**, 496-505 (1989).

Congwei L., Bin W., Zargari N. R., Devei X., Jiacheng W., *A Novel Three-Phase Three Leg AC/AC Converter Using Nine IGBT's*. IEEE Trans. on Power Electron., **24**, *5*, 1151-1160 (2009).

Do-Hyum Jang, Choe Ghy-Ha, Ehsany M., *Asymmetrical PWM Technique with Harmonic Elimination and Power Factor Control in AC Chopper*. IEEE Trans. on Power Electron., **10**, *2*, 175-184 (1995).

Jang D., Choe G., *Asymmetrical PWM Method for AC Chopper with Improved Input Power Factor*. IEEE PESC Conf. Rec., 1991, 838-845.

Kim J.H., Min B.D., Kwon B.H., Won S.C., *A PWM Buck-Boost AC Chopper Solving the Commutation Problem*. IEEE Trans. on Ind. Electron., **45**, *5*, 832-835 (1998).

Lai R., Wang F., Burgos R., Pei Y., Boroyevich D., Wang B., Lipo T.A., Immanuel V.D., Karimi K.J., *A Systematic Topology Evaluation Methodology for High-Density Three-Phase PWM AC-AC Converters*. IEEE Trans. on Power Electron., **24**, *7*, 1671-1681 (2009).

Li L., Yang Y., Zhong Q., *Novel Family of Single-Stage Three Level AC Choppers*. IEEE Trans. on Power Electron., **26**, *2*, 504-511 (2001).

Lucanu M., Ursaru O., Aghion C., *Single Phase AC Choppers with IGBT's*. Proc. of the Internat. Symp. on Signal, Circuits and Systems SCS 2003, July 10-11, 2003, 213-216.

Lucanu M., Ursaru O., Aghion C., *Single Phase AC Choppers with Inductive Load and Improved Efficiency*. Proc. of the Internat. Symp. on Signal, Circuits and Systems, ISSCS 2005, **2**, July 14-15, 2005, 597-600.

Neascu D.O., *Power Converter Topologies with Reduced Component Count for Automotive AC Auxiliary Power*. Signals, Circuits and Systems (ISSCS), 2013 Internat. Symp. on, DOI: 10.1109/ISSCS.2013.6651170, INSPEC Accession Number: 13879807, 11-12 July 2013, Iaşi, Romania, 1-4.

Revenkar G.N., Trasi D.S., *Symmetrical Pulse Width Modulated AC Chopper*. IEEE Trans. on Ind. Electron. Contr. Instrum., **IECI-24**, 1977, 41-45.

Thiago Soliero B., Clovis Petry A., Joao C. dos Fagundes S., Barbi Y., *Direct AC-AC Converters Using Commercial Power Modules Applied to Voltage Restorers*. IEEE Trans. on Ind. Electron., **58**, 1, 278-288 (2011).

Valachi A., Timis M., Danubianu M., *Some Contributions to to Synthesis and Implementation of Multifunctional Registers*. 11th WSEAS Internat. Conf. on Automatic Control, Modelling & Simulation (acmos'09), Istanbul, Turkey, May 30 - June 1, 2009, 146-149.

CONVERTOR AC-AC MONOFAZAT

(Rezumat)

Circuitul propus, alimentat în curent alternativ, are rolul de a converti tensiunea furnizată sarcinii, într-o tensiune alternativă, de aceeaşi alură, dar care se modifică conform caracteristicii de funcționare întâlnite în convertoarelor dc-dc de tip buck-boost (convertor mixt).

Strategia de comandă a tranzistoarelor din componența convertorului este simplă, managementului de control al gestionării energiei furnizate unei sarcini este mult simplificat, permițând pe ansamblu obținerea unor performanțe globale net superioare, față de managementul de control utilizat în topologiile clasice.